ISSN: 0369-8963

Examination of Microstructural Transformations and Tensile Attributes of Dissimilar Cda101–Aisi 1010 Joints Using Fsw Process

ANIL BASHA K[1#], SEVVEL P[2] AND GIRIDHARAN K[3]

[1]Assistant Professor, Dept. of Mechanical Engineering, GRT Institute of Engineering and Technology, Tiruvallur–631209, Tamil Nadu, India

[2] Professor, Department of Mechanical Engineering, S.A. Engineering College (Autonomous), Chennai – 600 077, Tamil Nadu, India

[3]Assistant Professor, Dept. of Mechanical Engineering, Easwari Engineering College (Autonomous), Chennai–600 089, Tamil Nadu, India

[#]Corresponding Author- ANIL BASHA K

Abstract:

Friction stir welding (FSW) was adopted to attain 3mm thick butt joints of flat plates of dissimilar metals namely CDA 101 and AISI 1010. Joints were fabricated by inserting a taper cylindrical tool pin at an offset of 1.5mm from the line of separation, towards the CDA101 plate at an 1100 rpm rotational speed & 35 mm/min tool travel speed, under a downward axial force of 7 kN. The microstructural transformations, tensile properties and phase constituents of the fabricated joints were examined and the results revealed, the joints were found to be free from flaws. Structural morphologies revealed that, CDA 101 side has encountered superior flow of the plasticized metal when compared with that of AISI 1010 side. SEM images exhibited the presence of intricate, infringed whirlpools, intertwined structures and associated patterns of material flow, thereby confirming a strong binding in nugget zone of nugget. Dissimilar joint exhibited UTS (ultimate tensile strength) of 181.5 MPa and 14.03% of elongation and the dissimilar joint's fractured specimen has failed under a brittle-ductile mode of fracture.

Keywords: *CDA 101; AISI 1010; Friction stir welding; Material Flow; Nugget zone; Mode of fracture*

Introduction

Welding of disparate materials is gaining worldwide attention, particularly in electronic, power & energy production, nuclear and petrochemical sectors, as there prevails a demand to obtain components with custom-built features and to acquire lightweight parts [1 – 3]. For instance, in recent years, needs have arisen for joining together alloys of copper (CDA101) and low carbon steel (AISI 1010) for use in various sectors especially for automotive components (Automotive rectifiers, transmission covers, pans, etc) and for the manufacture of various electrical parts (High resistance-ratio cryogenic shunts, transistor component bases, coaxial cables, coaxial tubes etc), as this combination of disparate materials will yield parts with exceptional strength at a reduced cost [4 – 6]. Yet, joining of disparate materials by regular & traditional joining processes will be a quite complex task, in view of their temperature of melting, the difference in composition, different physical nature and variations in stress, which will provoke imperfections including cracks, stresses (compressive, residual and thermal), corrosion etc [7, 8]. Apart from this, employing fusion based & traditional joining processes to join this disparate material combination (CDA101 & AISI 1010) will bring about severe damage in the zone of fusion, cracks at the interfaces of joint portions, as there exists a wide difference in thermal oriented physical features between CDA101 alloy & AISI 1010 alloy, inclusive of their point of melting, conductivity of heat, coefficient of expansion of heat etc., [9, 10]. So, there prevails an undeniable and immediate need for identification of a most suitable joining process for welding together CDA101 and AISI 1010, which will result in preferable quality

 https://doi.org/10.37896/pd91.5/91531

ISSN: 0369-8963

joints with minimum or negligible level of deterioration of those materials metallurgical and mechanical features [11, 12].

As techniques of solid-state joining (including forge based joining, friction-based joining, diffusion joining, ultrasonic based joining etc) can easily disentangle the issues of underlying welding irregularities & flaws, generated during the employment of traditional joining processes, they can be considered as effective methods for joining of this dissimilar material combination, namely copper (CDA101 grade) and low carbon steel (AISI 1010 grade) alloys [13, 14]. FSW (Friction stir welding) technique developed from the United Kingdom, has gained attraction worldwide in the past years and is considered as one of the most innovative & unique solid-state of welding processes. In this FSW process, the fluttering pin of the tool migrating at high speeds of rotation is infused into the region of joint of the materials to be welded together, till the tool's shoulder region comes into intimate interaction with the surfaces of those materials. Solid-state welding between the materials is achieved, as the materials at the region of the joint portion get softened, leading to the flow & mixing of the softened material under the coadjuvant impact of the heat by friction & stirring action by mechanical rotation of the tool pin [15 – 17].

Generation of lower volumes of temperature during joining, minimized joining duration, reduced input of heat are some of the unique & attractive features of this FSW technique and as a result, when FSW is employed for joining of disparate materials, it will efficaciously eliminate the majority of the flaws & defects associated with conventional fusion joining processes. In addition to this, FSW's reduced input of heat will also diminish the stresses (residual and thermal) and distortions, simultaneously leading to the attainment of uniquely refined microstructure together with high level of densification and assimilation, followed by substantial enhancement of the strength of the fabricated joints [18, 19].

In recent years, many investigational attempts were put forward successfully to join several dissimilar materials through the technique of FSW [20 – 30]. For example, Mohammadi et al. [20] experimentally proved, dissimilar lap joints of Al alloy (6061) and Mg alloy (AZ31B) can be obtained using the FSW technique. During this experimentation, joints were fabricated at tool speeds of travel and rotation ranging from 16 – 40 mm/min and 560-1400rev/min respectively. The specimen tensile shear test results revealed, maximum values of strength and ductility can be achieved by concurrent raise in the speeds of travel and rotation to 40 mm/min and 1400 rev/min respectively. Further investigation of the fractured surfaces proclaimed that the failure modes of these dissimilar joints were regulated by the intermetallic (brittle) compounds existing in the zone of nugget.

Joints between completely different materials namely low-carbon steel (St37) and stainless steel (304) were fabricated effectively by Ali Khodadadi et al. [22] by employing the technique of FSSW(friction stir spot welding) technique at tool speeds ranging from 630 rpm to 1250 rpm. Test reports indicated, the joints were found to be present with uniformly enhanced hardness values, which was due to the combined impact of the phase metamorphosis of the nugget region associated with St37 steel and the recrystallized nugget region of the 304 steel. It was also recorded that, the length of the bonding fabricated at larger speeds of rotation was found to be appreciable, contributing a 6682 N shear / tensile strength.

Galvao et al. [23] attempted to completely understand the binding structure between the Al – Cu and the failure mechanisms of these dissimilar joints (copper-DHP to 6082-T6 Al alloy) fabricated through FSW process and methodologically analyzed the impact of the offset (w.r.t tool) on the structural, mechanical and morphological properties of the fabricated weldments. It was experimentally recorded that, adopting the concept of offset w.r.t. tool position suppressed the formation of Cu/Al-based intermetallic compounds to greater extends, which have a strong tendency

 https://doi.org/10.37896/pd91.5/91531

ISSN: 0369-8963

to form internal detachment regions in the interior of nugget. Hence, the obtained joints of copper-DHP to 6082-T6 Al alloy were found to be present with desirable surface finish and quality.

Commercial brass (Cu-40Zn) was successfully welded with S25C grade carbon steel using FSW technique by Gao et al. [24] and it recorded the interconnectivity among the input of heat and the speed of joining. The variation in the speed of joining was found to have a major impact on the shear / tensile fracture load, size of the grains and hardness at the zone of stir of the fabricated joints. Further, observations made through electron (transmission) microscope and analysis of energy dispersive X-ray spectrometry proved, there existed a mutual region of diffusion of dominant elements (namely Zn, Fe & Cu) at the interface of the joints, fabricated at 500 mm/min travel speed, which eliminated the formation of intermetallic compounds.

Barlas et al. [26] exhibited the practicability of welding together a dissimilar sheet of brass (CuZn30) to a commercially pure copper sheet by FSW. The results of the conducted bending and tensile tests conceded, the joints strength of bend was nearly 31% minimal and 47% greater than their parent metals i.e., brass and pure copper respectively. Detailed analysis of the microstructural zones portrayed the presence of regranulated grains of brass and insinuated vortex, swirl-like formations in the center region of the zone of nugget, characterizing the presence of Cu layers and regranulated grains of brass.

In addition to this, Li et al. [27] performed an investigation to join sheets (2mm) of 30CrMnSiNi2A (medium carbon steel) and Ti6Al4 V (Titanium alloy) at a fixed 750 rpm rotating speed and at speeds of travel ranging from 47.5 – 75 mm/min. This investigation affirmed, the interfacial layer's thickness declines with the gradual rise of the speed of tool travel. In better words, the joints fabricated at 75 mm/min travel speed exhibited the presence of 1 μm thick interfacial layer and an interfacial layer having ~5 to 60 μm thickness was found in the joints obtained at 47.5 mm/min. Defect-free weldments experienced fracture at region influenced by thermal stresses to region influenced by heat on surface of carbon steel or at layer of interfacial reaction on the titanium region.

The impact of the various parameters of the FSW technique namely position of tool pin, rate of tool rotation, speed of tool travel on tensile and structural features of the joints during FSW of 6061 Al alloy and Ti6Al4V alloy was investigated by Wu et al. [29]. The recorded observations declared, the rate of tool rotation determines the strength (tensile) and location of fracture of the joints. Moreover, the joints fabricated at 750 rpm were found to possess a 100 nm thick TiAl3 Intermetallic compounds at the region of interface and this joint exhibited a strength of 215 MPa (i.e., nearly 68% of the strength of base material – 6061 Al) and the fracture occurred at the heat affected region and thermo-mechanically affected region of the 6061 Al alloy.

In the category of immiscible metal combination, an innovative attempt was made by Won et al. [30] to join pure magnesium and pure titanium plates. The joint obtained at optimized values of probe offset & speed of joining exhibited uppermost tensile strength (150 MPa), approximately 88% of the strength of pure Mg and was characterized by the occurrence of the fracture at the heat affected region of the Mg. This fracture mechanism confirmed the establishment of the thin layer of intermetallic compounds at the interface of the weld and the resistance to the development of intermetallic elements (brittle natured) in marrow of zone of stir of Mg.

From these various literature reviews, it must be highlighted that, so far, most of the worldwide experimental attempts by several researchers have been made to join a disparate metal combination of Al to Cu, Al to Mg, Ti to Al, brass to steel, pure copper to brass, Ti to medium carbon steel, Ti to Mg only, using the technique of FSW. Even though there exists an urgent demand in the current industrial scenario, for obtaining components with copper & steel dissimilar metal

 https://doi.org/10.37896/pd91.5/91531

ISSN: 0369-8963

joint, exhibiting unique properties like improved strength, better electrical conductivity & resistivity etc., at a reduced cost, to the premium of investigator's awareness, joining of an immiscible metal combination of the alloy of copper (CDA101) and low carbon steel (AISI 1010) by FSW technique has never been reported. Hence, it becomes indispensable to carry out an experimental attempt to join the divergent metal joint of CDA101 and AISI 1010 using the technique of FSW.

Materials arrangement and experimental frame-up

Plates of the alloy of copper namely CDA101 and low carbon steel namely AISI 1010 of 3 mm thickness were used in this investigation. Table 1 describes the chemical configuration of base metals namely CDA 101 and AISI 1010. Heretofore to the joining of these materials by FSW technique, the flat plates were shaped into perfect plates possessing dimensions of 50 mm (width) and 100 mm (length). The entire regions of those two unalike material flat plates are rubbed slightly with the paper of grit and then cleansed with ethanol to remove any impurities or foreign particles.

Table 1. Chemical Configuration of CDA 101 and AISI 1010 alloy plates investigated in this work

Material of Investigation	**Zn**	**Fe**	**Pb**	**Cr**	**Si**	**Ni**	**S**	**P**	**less than <0.001**	**Cu**
CDA 101	0.014	<0.016	<0.005	<0.01	<0.005	<0.005	<0.002	<0.005	Mn, Al, Sn, Mg	Balance
Material of Investigation	**W**	**Al**	**Mn**	**Mo**	**Cr**	**P**	**Ni**	**Cu**	**Si**	**Fe**
AISI 1010	0.05	0.05	0.22	0.013	0.012	0.022	0.021	0.021	0.011	Balance

Arrangement of the materials during the joining process by FSW technique with a flat plate of CDA101 placed on the side of advancement (AS) of the tool and flat plate of AISI 1010 placed on the side of retreating (RS) of the tool is graphically illustrated in Fig. 1. Tungsten carbide (WC) based tool was employed in this investigation and it consisted of a 25mm (diameter) cylindrical outer shoulder, 12 mm (diameter) cylindrical inner shoulder along with a taper cylindrical-shaped pin (2.85 mm in length). The tool was introduced into the CDA101 flat plate at about 1.5 mm offset from the line of separation of the two plates as seen in this Figure 1 under a downward axial force of 7 kN, rotating at 1100 rpm and speed of travel of the tool was 35 mm/min in the direction being similar to the orientation of involution of the flat plates. The full length of the taper cylindrical pin (i.e., 2.85 mm) was made to penetrate completely into the flat plates and was made to travel to the entire length of the flat plates, in the above described joining conditions.

After the fabrication of the weldments of unalike CDA 101 and AISI 1010, the weldments were analyzed and the analysis of their macro, microstructural images were carried out on their cross-section exactly at right angles to the direction of their joining. Macro structures and microstructures of these joints were analyzed with the help of Optical Stereo Microscope (Stereo discovery type) and these joints scanning electron microscopic (SEM) images were obtained using a FEI Quanta High Resolution Scanning Electron Microscope equipped together with a system of EDX. Measurements

 https://doi.org/10.37896/pd91.5/91531

ISSN: 0369-8963

for Vickers hardness were executed using a Tv-50 model computerized Vickers Hardness Tester at the lower, center & upper regions across the zone of weld in a 3 X 22 cluster at hiatus of 0.2 mm vertically and 1 mm horizontally under a 0.98 N load for a time of dwell of 15 seconds. Specimens for the test of tensile were elicited vertically to the direction of joining as per the ASTM – E8 standards with gauge length of 25mm. Tests related to tensile were executed at normal temperature under 1.5 mm/min crosshead speed.

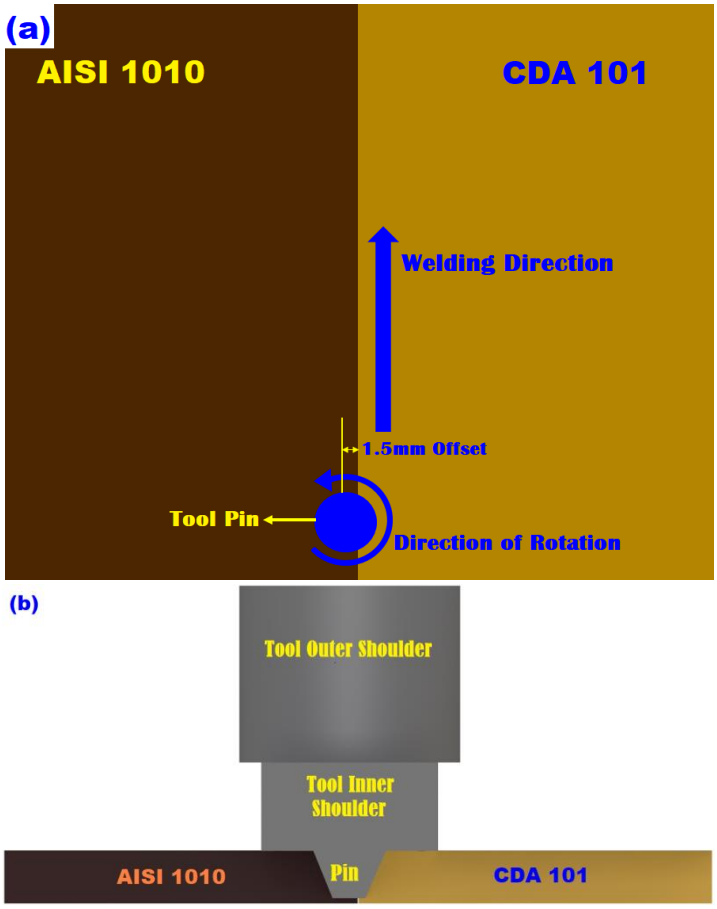

Figure 1. (a) and (b). Diagrammatic illustration of the various views of the materials arrangement during the joining of flat plates by FSW process

Examinations, Interpretations and Outcomes

Observations on Surface morphology, Macro structures

Different photographic views of the surface morphology of a fabricated dissimilar joint of CDA 101 and AISI 1010 are shown in Fig.2.

https://doi.org/10.37896/pd91.5/91531

ISSN: 0369-8963

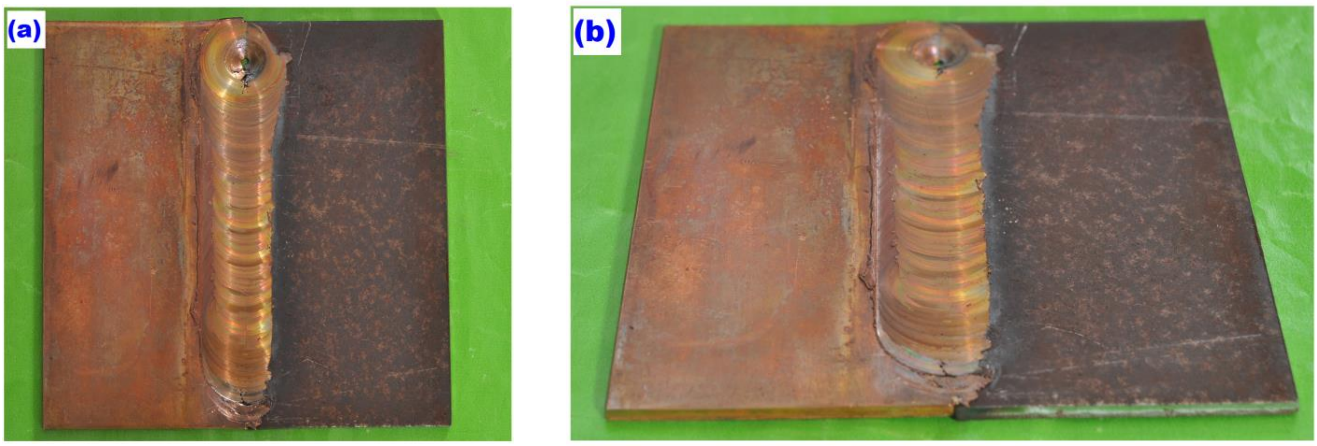

Figure 2. (a) and (b). Different photographic views of the surface morphology of the fabricated dissimilar joint of CDA 101 and AISI 1010

It can be conceived, the flat plate of CDA 101 placed has encountered superior flow of the plasticized metal when compared with that of AISI 1010, at the equivalent processing temperature. This is mainly due to the reason, low carbon steel (i.e., AISI 1010) possesses higher values of melting temperature, hardness, tensile strength than the copper alloy (CDA 101). An additional reason for this superior flow is, we have introduced the pin of the tool in the side of copper flat plate with an offset of 1.5 mm from the line of separation. And due to this, the fabricated unalike CDA 101 & AISI 1010 joints have experienced a bountiful supply of the plasticized material during the tool travel.

At the same time, if the joints have been formed by introducing the tool exactly at the line of separation of the two plates, without any offset, the joints would have been found with various flaws including keyholes, grooves etc., resulting from non-uniform flow of the softened material [31, 32]. In the above surface morphology photographs, we can observe, the region of the joint is enshrouded by a coat of copper material and some flickers can be seen at the borders of the joint. Even though, the fabricated joint seems to be flawless, by closely observing its surface morphology, to confirm the absence of defects, macrostructural image of this joint was obtained and is illustrated in Fig.3. From this Fig.3, it can be noted, the center of the joint region, i.e., the zone of nugget is found to be free from flaws and it is composed of elements of both copper and low carbon steel. Moreover, the structure of this zone of nugget seems to be very much distinctive, due to the flow of the divergent materials.

Figure 3. Macrostructural image of the fabricated dissimilar joint of CDA 101 and AISI 1010

Inferences from Microstructural images

To completely understand the pattern and manner, in which the flow of the softened materials and phase transformations have occurred, microstructural images of various zones of this specimen were recorded and are illustrated in Fig. 4(a)–(h). The various regions of the fabricated dissimilar CDA101 and AISI 1010 were categorized into four zones namely stir zone, thermo-mechanically affected zone, heat affected zone and base metal and all these zones of the fabricated joint are clearly illustrated in Fig. 4(a)-(h). As seen in Fig. 4(a), microstructure of the base metal copper plate (i.e., CDA101) is found be present with large equiaxed grains of Cu with precipitated cuprous oxide at the grain boundaries. The size of the grains is in the range of 28 – 30 microns. The

https://doi.org/10.37896/pd91.5/91531

ISSN: 0369-8963

microstructure also reveals the presence of some twinned grains formed during the cold forming of the plate. Fig. 4(h) illustrates the microstructure of another base metal, namely low carbon steel plate (i.e., AISI 1010) possessing grains of pearlite in ferrite matrix. The pearlite grains are found to be present at the grain perimeters of ferrite. The flow of grains had occurred along the direction of forming of the plate and the grain size falls within the range of 38 – 40 microns.

Fig. 4 (b) and (g) represents the heat affected zone of in the CDA101 and AISI 1010 sides respectively. The common feature of these two zones of CDA101 and AISI 1010 is, plastic deformation has not happened and the grains have been subjected to frictional heat kindling them to grow. When compared with that of their base metals, it can be noted, the structure of the grains in both the zones w.r.t. their respective base metal grain structure have not modified much, but at the same time, the grains in both the heat-affected zones have become coarser, due to the impact of the thermal cycle. Fig. 4(c) portrays the thermo-mechanically affected zone on CDA101 side, where the grains have been influenced by the stirring action of the employed tool pin and frictional heat, which have impacted the grains in this zone to go through noteworthy plastic deformation [33]. It can also be seen, the grain in this zone has experienced grain orientation along the direction of the flow of the softened material (Cu constituents).

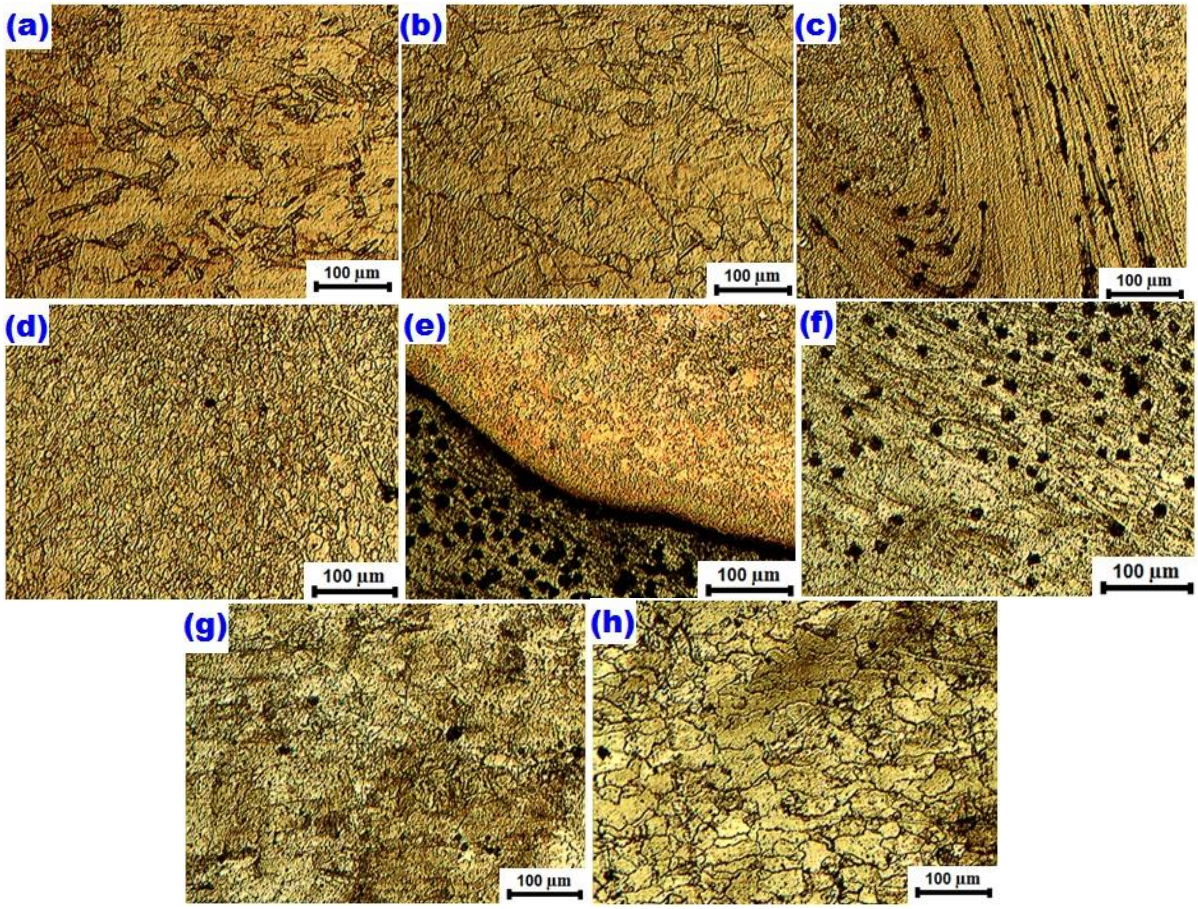

Figure 4. Optical microstructural images of various regions of the fabricated dissimilar joint of CDA 101 and AISI 1010 namely (a) Base metal: CDA 101 (b) Heat affected zone on CDA101 side (c) Thermo-mechanically affected zone on CDA101 side (d) stir zone on CDA101 side (e) Interface junction at stir zone (f) stir zone on AISI 1010 side (g) Heat affected zone on AISI 1010 side (h) Base metal: AISI 1010

Fig. 4 (e) reveals the interface junction at the nugget zone where the constituents of copper and steel constituents had occurred. The left is the steel matrix and the right is the copper matrix. The fusion/zone line can be seen to be enriched with copper metal. The steel zone shows fine

 https://doi.org/10.37896/pd91.5/91531

ISSN: 0369-8963

fragmented grains of pearlite in ferrite matrix with typical low carbon steel. The copper side had undergone severe plasticity and can be confirmed by the substantial flow of copper metal. Fig. 4(f) describes the stir zone in AISI 1010 (low carbon steel) side, which can be seen to have undergone fragmentation and have resulted in the reduction of the size of the grains. In addition to this, this zone is also found to possess the presence of the infiltrated copper particles & their dispersions.

The stir zone in CDA101 side is shown in Fig. 4(d). In this image, it can be ascertained that, due to the mixed impact of the frictional heat & downward axial force exerted on the tool, the grains in this zone have undergone a complete transformation in their size and shape. They have been transformed & disintegrated into fine re-crystallized grains, measuring to the size of 10 – 13 microns and the presence of such disintegrated grains in the stir zone with reductions in their size & uniform distribution is a proven fact, that sound quality joints have been achieved [34, 35].

Perceptions of SEM images

The above mentioned macro structural and microstructural images have already revealed, the major portion of the nugget Zone of the fabricated joint comprises copper and the ingredients of steel have scattered in that zone in different shapes. This was mainly due to the insertion of the pin of the tool at an offset of 1.5mm towards the CDA 101 plate side. At the same time, the amalgamation of the copper and steel (i.e., ingredients of CDA 101 and AISI 1010) is very much arduous to understand. Moreover, we can observe the presence of diverse microstructures in the various regions of the fabricated joint, especially in and around the nugget zone. So, to have a better understanding of the flow of these softened materials, their distribution in various regions and to characterize the structures of the above-mentioned zones of the fabricated dissimilar joint of CDA 101 and AISI 1010, SEM images, shown in the Fig. 5 (a) – (i) were analyzed.

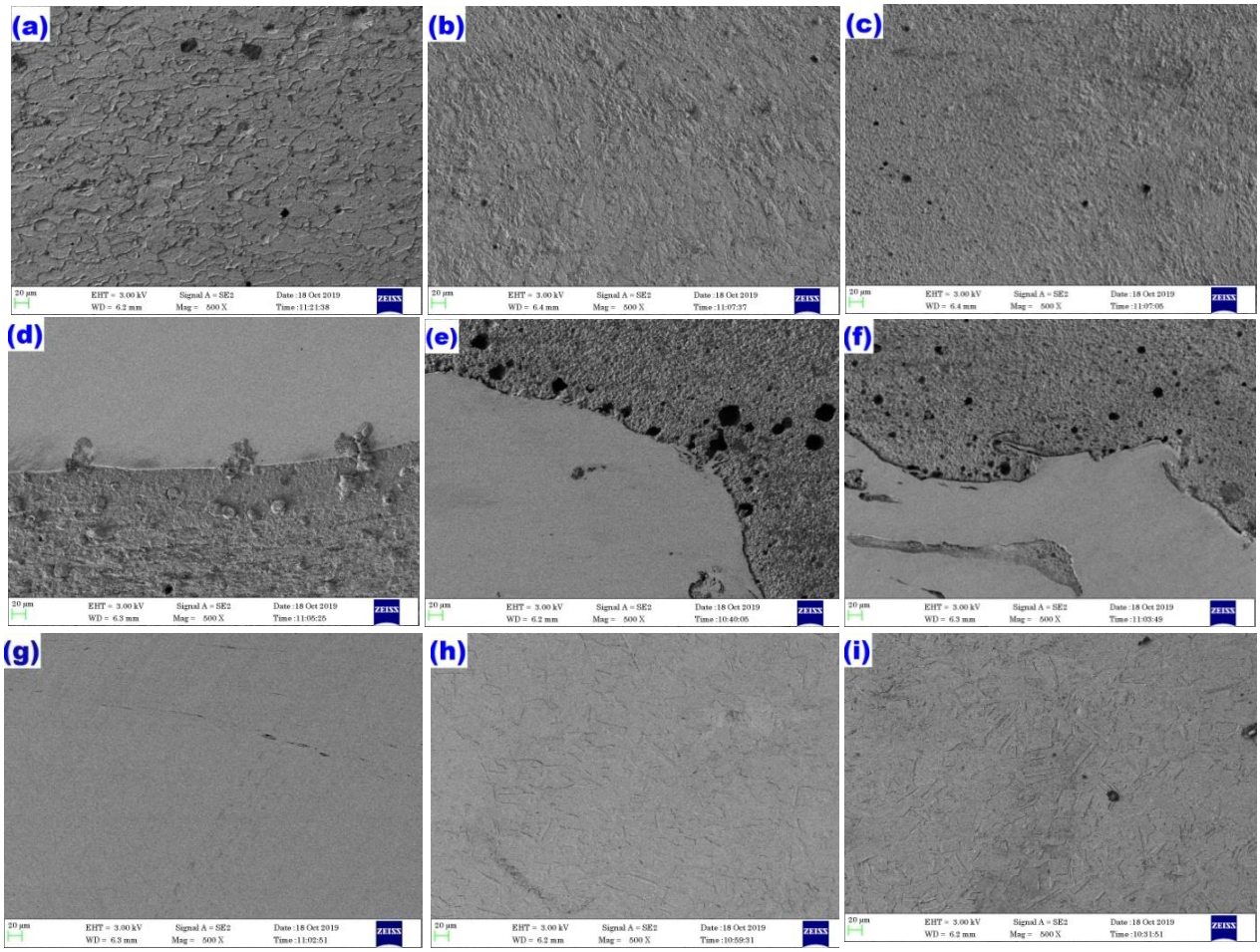

Figure 5. Images of SEM revealing various regions of the fabricated dissimilar joint of CDA 101 and AISI 1010 namely (a) Base metal: AISI 1010 (b) Heat affected zone on AISI 1010 side (c)) stir

https://doi.org/10.37896/pd91.5/91531

ISSN: 0369-8963

zone on AISI 1010 side (d) bottom portion of interface zone of CDA 101 and AISI 1010 (e) region of interconnection of two distinct microstructural constituents of Cu & steel (f) interface fusion zone of CDA 101 and AISI 1010 (g) stir zone on CDA 101 side (h) Heat affected zone on CDA 101 side (h) Base metal: CDA 101

Fig. 5(a) displays us the SEM micrograph of base metal of low carbon steel (i.e., AISI 1010), which contains elongated grains of pearlite in ferrite matrix along the direction of forming of the plate and the size of the grains in the region measures to be in the range of 38 – 40 microns. Fig. 5(b) shows the heat-affected zone on the AISI 1010 plate. In this zone, we can observe, the grains appear to be finer than the grains present in the base metal region and they also appear to be recrystallized and the grains size is reduced to 30 microns approximately, which have occurred due to the impact of the developed frictional heat. Fig. 5(c) represents the nugget region of the AISI steel matrix. It can be visualized that, frictional heat and thermal stresses have resulted in the dissolution and recrystallization of the constituents of the AISI 1010 steel, consisting of completely fine grains of pearlite dispersed in ferrite matrix [6, 36].

The bottom portion of the interface zone of CDA101 copper and AISI 1010 steel is described in Fig. 5(d). The bottom portion of this image shows the heat affected region of the AISI 1010 steel and the top portion shows the nugget region of the CDA 101 Copper matrix. It can be noticed, the grains of copper have transformed into very much finer size along with substantial plasticity of copper constituents. In addition to this, this interface zone reveals the fusion of constituents of two dissimilar metals. i.e., the diffusion of AISI 1010 steel particles into the matrix of copper. Likewise, Fig. 5(e) shows the bonding & flow between the microstructural constituents of two completely dissimilar metals, i.e., CDA 101 & AISI 1010. On the left side of this image contains the region of copper and the right side contains the nugget region of the AISI 1010 steel. It can be witnessed that, there exists an appreciable volume of fusion among these dissimilar metals and we can observe the diffusion of AISI 1010 steel particles into the CDA 101 copper matrix at the interface fusion region.

The interface fusion zone of CDA 101 copper and AISI 1010 steel exactly nearer to the nugget zone is illustrated in Fig. 5(f). From this image, it can be understood, the materials on the portion of CDA101 have experienced plastic deformation at higher degrees and these softened materials due to tool pin's stirring action have travelled to the other side (AISI 1010) of the plate [5, 18]. This flow of the plasticized & softened materials of CDA 101 has resulted in the formation of alternate layers around the steel (AISI 1010) matrix. Fig. 5(g) represents the nugget region of the CDA 101 copper. This region contains fine fragmented and re-crystallized grains, which have achieved this state due to the combined actions of the downward force exerted axially on the rotation tool pin and the heat of friction provoked by the continuous contact of shoulder of tool with metal plates [13, 37].

The heat-affected region on CDA 101 side is shown in Fig. 5(h). In this region, we can observe, the grains of the copper constituents have experienced high temperature & thermal stresses due to the developed frictional heat, which has made the grains in this region to be coarser, without much modification in their shape and structure. The SEM image of another base metal i.e., CDA 101 is displayed in Fig. 5(i) and is found to possess constituents of Cu with precipitated cuprous oxide (Cu2O) at the grain boundaries, along with some twinned grains, which have been formed during the cold forming of the plate. Apart from this, we can visualize the presence of apical horizon amidst the base material (AISI 1010) and the nugget zone on the steel side, while this line of separation between CDA101 & its nugget zone is not as noticeable as that of the steel side. The intertwined structure formed by copper and steel constituents, (as seen in these SEM images) reveals, the existence of strong binding in this region [38]. In these SEM images, we can observe the presence of

 https://doi.org/10.37896/pd91.5/91531

ISSN: 0369-8963

intricate, infringed whirlpools and associated pattern of material flow, confirming the occurrence of convolute inter dispersion and merging of the constituents of two different materials, which is a strong evidence for the fact that, an effective joining of dissimilar materials have taken place [39, 40].

Scrutiny of EDX images

Results of the chemical microanalysis of the energy dispersive X-Ray spectroscopy (EDX) test performed at the interacting zone of fabricated CDA 101 and AISI 1010 joint are graphically illustrated in Fig. 6(a-c). We observe that the X-ray spectrum has been focused towards the nugget region containing the zone of fusion of the constituents of the dissimilar metals namely copper (CDA101) and steel (AISI 1010) and this zone has been marked clearly by a pink-colored rectangular box as seen in the Fig. 6(a). The percentage of the various elements detected in this region is graphically illustrated in the Fig. 6(b) and the same is numerically described in the Fig.6(c), in the form of a tabular column, mentioning the values of various present elements both in weight and in atomic percentages.

Fig. 6 (b) reveals us the presence of copper, iron, oxygen and carbon in the focused interface region of the fabricated dissimilar joint and their percentage of weight being 52.24 % for copper, 38.57 % for iron (i.e., steel), 3.14% of oxygen and 6.05% of carbon. The presence of oxygen constituents reveals that, oxidation between the matrix of copper and steel (iron) has occurred in this region. We can also observe, the dominant constituent in this part is copper when compared with that of the steel (iron) and the reason for this is, the constituents of copper (CDA 101 base metal plate) have undergone a high level of plastically deformation, resulting in a large volume of softened material of the copper side, by virtue of insertion of the pin of operated tool towards CDA101 side, with an offset of 1.5 mm from the line of joint [16, 21]. Then, the combined impact of the stirring action of pin & the axial force exerted on the pin must have forced these softened materials of copper constituents to flow towards the other region of the plate.

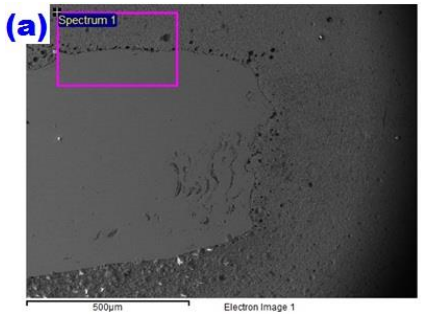

(c)

Element	Weight%	Atomic%
O	3.14	8.88
C	6.05	22.76
Fe	38.57	31.21
Cu	52.24	37.16
Total	100.00	

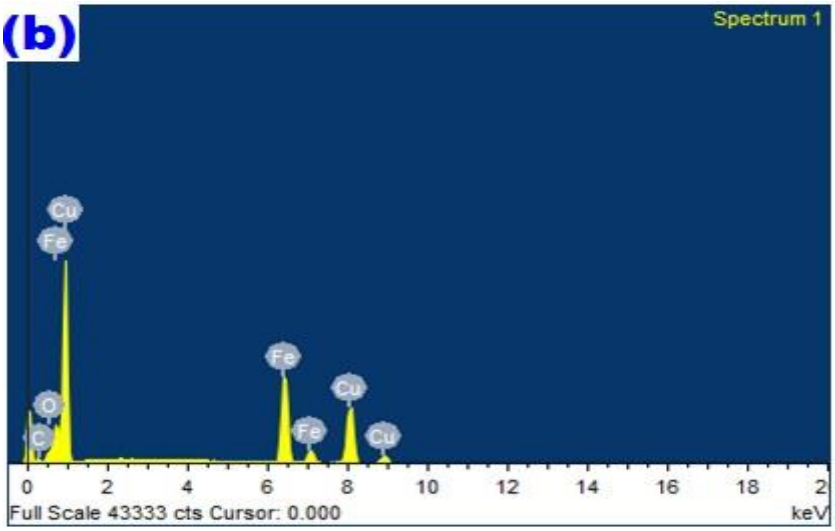

Figure 6. (a) Interface region of the fabricated dissimilar joint of CDA 101 and AISI 1010 observed during EDX test (b) Graphical representation of the various elements detected in the focused interface region during the EDX test and (c) Numerical description of the weight and atomic percentage of the various elements being present in the focused interface region

https://doi.org/10.37896/pd91.5/91531

ISSN: 0369-8963

At the same time, from the XRD graphs, we cannot locate the presence of any copper - steel intermetallic compounds, which is an indication, phase transformations between copper – steel have not taken place during the fabrication of dissimilar joints of CDA101 and AISI 101, as mentioned by several researchers [17, 41, 42]. A Major reason for the absence of these intermetallic compounds is, the time of hold at peak temperatures is very much shorter during the FSW of thin plates (as in our case of 3mm), because of the faster rate of cooling [30, 43]. Hence, the time of diffusion was not sufficient enough to promote the formation of the copper – steel intermetallic compounds.

Tensile Fractography

The tensile properties of the base metals of this experimental investigation (i.e., CDA 101 and AISI 1010) and the fabricated dissimilar joint are illustrated in Table 2. From this table, it can be seen that, the strength of the fabricated dissimilar joints is comparatively satisfactory, exhibiting UTS (ultimate tensile strength) of 181.5 MPa, which is 77.6% of the strength of the CDA101 base metal. The corresponding value of elongation for that fabricated joint is 9.4%.

Table 2. Tensile properties of the dissimilar base metals and the fabricated dissimilar joint

Material of Investigation	Tensile Strength	Yield Strength	Elongation
CDA 101	234 MPa	207 MPa	14 %
AISI 1010	365 MPa	305 MPa	20 %
CDA 101 – AISI 1001 dissimilar joint	181.5 MPa	107.04 MPa	14.03 %

This confirms the fact that, the strength of the dissimilar joints fabricated by FSW technique is customarily lesser than that of their parent materials, due to their inhomogeneous microstructures [10, 44]. The photograph of the fractured tensile specimen of the fabricated dissimilar joint is displayed in Fig.7. In this figure, it can be noticed that, almost all the tensile specimen have undergone fracture in their Cu (CDA 101) side of the nugget region and petting can also be seen in the fractured specimen, implying us that, there exists a tenacious bonding between the dissimilar CDA 101 and AISI 1010 materials, because of employment FSW technique.

Figure 7. Photograph of the fractured tensile specimen of the fabricated dissimilar CDA 101 and AISI 1010 joint

To obtain a better understanding of the modes in which fracture has occurred in these tensile specimens, they were examined through scanning electron microscopy and the obtained SEM images of these tensile specimens are illustrated in Fig. 8 (a)–(e). SEM photographs of the tensile fractured portion of the specimen can be seen in Fig. 8(a). This image illustrates the entire zone of

 https://doi.org/10.37896/pd91.5/91531

ISSN: 0369-8963

the fracture with copper at its top portion and the matrix of steel at its bottom portion. The copper side has undergone a ductile mode of fracture with finer grains possessing a higher level of plasticity. At the same time, we can see that the steel matrix at the bottom portion has experienced less flow of the plasticized grains.

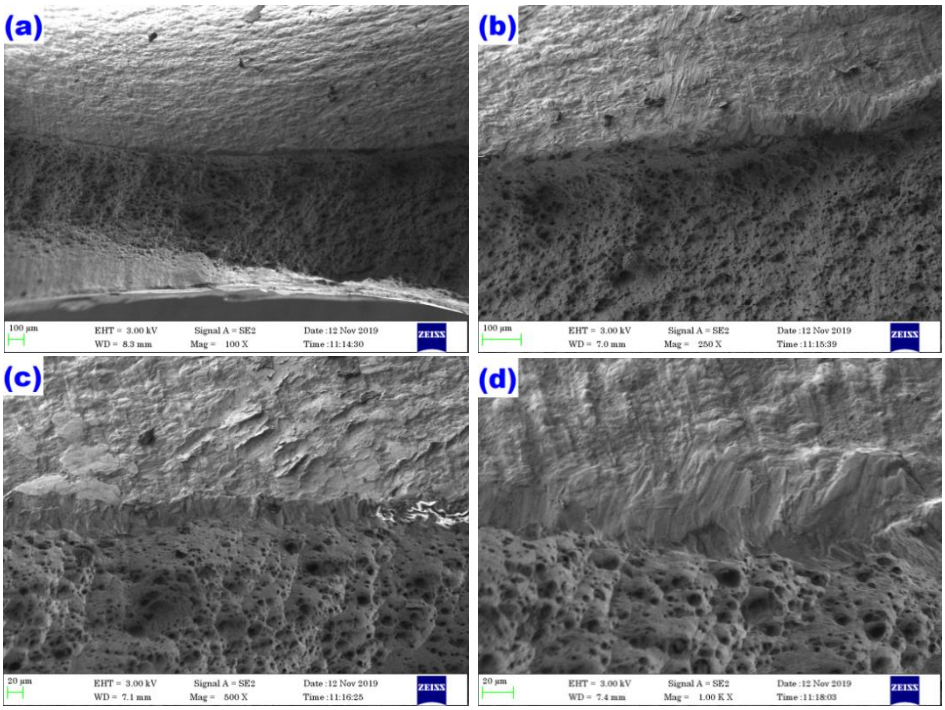

Figure 8. SEM images of the fractured tensile specimen of dissimilar CDA 101-AISI 1010 joint fabricated by FSW

Fig. 8 (b) – (d) portrays the magnified images of the center region of the fractured portion at different magnification levels, in which we can observe the zone of fusion of the two dissimilar materials, i.e., copper (at the top) and steel (at the bottom). The steel matrix at the lower portion in the magnified form is found to exhibit lower levels of plasticity. At the same time, the morphology of the fractured surface containing copper is found to show higher levels of elongation, due to the finer sized grains, resulting from substantial & dense flow of softened material, due to which the fusion zone was found be free from voids.

As a result of this, the fractured surface features are found to vary considerably with locations across the joint and the intricate nugget zone microstructure has also contributed to this location of fracture surfaces [25, 45]. In addition to this, we can notice the presence of a large number of small dents with varying depths at the bottom of the fracture surface i.e., in the steel matrix region, which might have occurred due to lower plasticity and hence we cannot observe any yielding at the steel matrix. So, we can resolve that, the mode of fracture of the tensile specimen of this dissimilar joint is a mixed brittle–ductile mode of fracture.

Conclusions

The technique of FSW was employed to accomplish the butt joints of divergent materials namely CDA 1010 and AISI 1010. Examinations were performed on fabricated dissimilar joints and the examination results are epitomized as listed below:

- Flawless, preferable quality dissimilar joints of CDA 101 and AISI 1010 were successfully obtained by rotating tool at 1100 rpm & 35 mm/min travel speed in the direction being similar to the orientation of involution of the flat plates, under a downward axial force of 7 kN, by employing a tool possessing taper cylindrical pin.

 https://doi.org/10.37896/pd91.5/91531

ISSN: 0369-8963

- Macrostructural surface morphology revealed that, the CDA 101 side has encountered superior flow of the plasticized metal when compared with that of AISI 1010 side, at the equivalent processing temperature. The reason for this superior flow of copper is the insertion of the tool pin at an offset of 1.5 mm from the line of separation of the two plates, towards the CDA101 plate side.
- The fusion/zone line at the center of the nugget was found to be enriched with copper. The steel matrix exhibited fine fragmented grains of pearlite in ferrite matrix with typical low carbon steel. The copper side had undergone severe plasticity, confirmed by the substantial flow of copper metal.
- The grains in the stir zone of CDA101 were found to have undergone a complete transformation in their size and shape, by the mixed impact of the frictional heat & downward axial force exerted on the tool. They have been transformed & disintegrated into fine re-crystallized grains, measuring to the size of 10 – 13 microns and the presence of such disintegrated grains in the stir zone with reductions in their size & uniform distribution proved that sound quality joints have been achieved.
- Intertwined structure formed by copper and steel constituents, (as seen in these SEM images) revealed the existence of strong binding in the nugget zone. In these SEM images, the presence of intricate, infringed whirlpools and associated patterns of material flow were noticed, confirming the occurrence of convolute inter dispersion and merging of the constituents of two different materials, a strong evidence for the effective joining of dissimilar materials have taken place.
- From XRD graphs, the presence of copper - steel intermetallic compounds cannot be located, which indicates, phase transformations between copper – steel have not taken place during the fabrication of dissimilar joints of CDA101 and AISI 101.
- The strength of the fabricated dissimilar joints was comparatively satisfactory, exhibiting UTS (ultimate tensile strength) of 181.5 MPa, which is 77.6% of the strength of the CDA101 base metal. The corresponding value of elongation for that fabricated joint was 14.03 % and the dissimilar joint’s fractured specimen failed under a brittle-ductile mode of fracture.

References

1. K. P. Mehta, V. J. Badheka, “A review on dissimilar friction stir welding of copper to aluminum: process, properties, and variants”, Materials and Manufacturing Processes, **31(3)**, 233−254 (2016)
2. B.P. Logan, A.I. Toumpis, A.M. Galloway, N.A. McPherson, S.J. Hambling, “Dissimilar Friction Stir Welding of Duplex Stainless Steel to Low Alloy Structural Steel”, Science and Technology of Welding and Joining, **21**, 11–19 (2016).
3. V.J. Badheka, R. Basu, J. Omale, J. Szpunar, “Microstructural aspects of TIG and ATIG welding process of dissimilar steel grades and correlation to mechanical behavior”, Transactions of The Indian Institute of Metals, **69** 1765–1773 (2016)
4. S. Yaknesh, K. Sampathkumar, P. Sevvel P, “Effect of Tool Pin Geometry and Process Parameters During FSW of Dissimilar Alloys of Mg”, Materials Research–Ibero–American Journal of Materials, **25**, e20210508 (2022)
5. A. Esmaeili A, H. Z. Rajani, M. Sharbati, M.B. Givi, M. Shamanian, “The role of rotation speed on intermetallic compounds formation and mechanical behavior of friction stir welded brass/aluminum 1050 couple”, Intermetallics, **19(11)**, 1711−1719 (2011)

 https://doi.org/10.37896/pd91.5/91531

ISSN: 0369-8963

6. H. Vashishtha, R.V. Taiwade, S. Sharma, A.P. Patil, "Effect of welding processes on microstructural and mechanical properties of dissimilar weldments between conventional austenitic and high nitrogen austenitic stainless steels", Journal of Manufacturing Processes, **25**, 49–59 (2017).
7. M. Kimura, K. Kasuya, M. Kusaka, K. Kaizu, A. Fuji, "Effect of friction welding condition on joining phenomena and joint strength of friction welded joint between brass and low carbon steel", Science and Technology of Welding and Joining, **14**, 404–412 (2009).
8. D.M. Sekban, S.M. Aktarer, P. Xue, Z.Y. Ma, G. Purcek, "Impact Toughness of Friction Stir Processed Low Carbon Steel Used in Ship building", Materials Science and Engineering: A, **672**, 40–48 (2016)
9. H. Barekatain, M. Kazeminezhad, A. Kokabi, "Microstructure and mechanical properties in dissimilar butt friction stir welding of severely plastic deformed aluminum AA 1050 and commercially pure copper sheets", Journal of Materials Science and Technology, **30(8)**, 826−834 (2014)
10. K. Giridharan, P. Sevvel, B. Stalin, M. Ravichandran, P. Sureshkumar, "Microstructural Analysis and Mechanical Behaviour of Copper CDA 101/AISI-SAE 1010 Dissimilar Metal Welds Processed by Friction Stir Welding", Materials Research Ibero-american Journal of Materials, **25**, e20210430 (2022)
11. M.N. Esfahani, J. Coupland, S. Marimuthu, "Microstructure and mechanical properties of a laser welded low carbon-stainless steel joint", Journal of Materials Processing Technology, **214**, 2941–2948 (2014)
12. N. Arivazhagan, S. Singh, S. Prakash, G.M. Reddy, "Investigation on AISI 304 austenitic stainless steel to AISI 4140 low alloy steel dissimilar joints by gas tungsten arc, electron beam and friction welding", Materials & Design, **32**, 3036–3050 (2011)
13. L. Zhou, R.X. Zhang, G.H. Li, W.L. Zhou, Y.X. Huang, and X.G. Song, "Effect of Pin Profile on Microstructure and Mechanical Properties of Friction Stir Spot Welded Al-Cu Dissimilar Metals", Journal of Manufacturing Processes, **36**, 1–9 (2018)
14. C. Satheesh, P. Sevvel, R. Senthil Kumar, "Experimental Identification of Optimized Process Parameters for FSW of AZ91C Mg Alloy Using Quadratic Regression Models", Strojniski Vestnik / Journal of Mechanical Engineering, 66 (12), 736 – 751 (2020)
15. D. Kumar, G. Sahoo, R. Basu, V. Sharma, M.A. "Mohtadi-bonab, Investigation on the Microstructure—Mechanical Property Correlation in Dissimilar Steel Welds of Stainless Steel SS 304 and Medium Carbon Steel EN 8", Journal of Manufacturing Processes, **36**, 281–292 (2018).
16. K. Giridharan, P. Sevvel, C. Gurijala, B. Yokesh Kumar, "Biochar-assisted copper-steel dissimilar friction stir welding: mechanical, fatigue, and microstructure properties", Biomass Conversion and Biorefinery, (2021)
17. P. Upadhyay, A.P. Reynolds, "Effects of thermal boundary conditions in friction stir welded AA7050-T7 sheets", Materials Science and Engineering: A, **527**, 1537–1543 (2010)
18. G. Sharma, D.K. Dwivedi, "Study on microstructure and mechanical properties of dissimilar steel joint developed using friction stir welding", International Journal of Advanced Manufacturing Technology, **88**, 1299–1307 (2017)
19. S.D. Dhanesh Babu, P. Sevvel, R. Senthil Kumar, V. Vijayan, J. Subramani, "Development of Thermo Mechanical Model for Prediction of Temperature Diffusion in Different FSW Tool Pin Geometries During Joining of AZ80A Mg Alloys", Journal of Inorganic and Organometallic Polymers and Materials, **31 (7)**, 3196–3212 (2021)

 https://doi.org/10.37896/pd91.5/91531

ISSN: 0369-8963

20. J. Mohammadi, Y. Behnamian, A. Mostafaei, H. Izadi, T. Saeid, A. H. Kokabi, A. P. Gerlich, "Friction stir welding joint of dissimilar materials between AZ31B magnesium and 6061 aluminum alloys: Microstructure studies and mechanical characterizations", Materials Characterization, **101**, 189–207 (2015)
21. A.Heidarzadeh, H. M. Laleh, H. Gerami, P. Hosseinpour, M. J. Shabestari, R. Bahari, "The origin of different microstructural and strengthening mechanisms of copper and brass in their dissimilar friction stir welded joint", Materials Science and Engineering: A, **735**, 336–342 (2018)
22. A. Khodadadi, M. Shamanian, F. Karimzadeh, "Microstructure and Mechanical Properties of Dissimilar Friction Stir Spot Welding Between St37 Steel and 304 Stainless Steel", Journal of Materials Engineering and Performance, **26**, 2847–2858 (2017)
23. I. Galvão, A. Loureiro, D. Verdera, D. Gesto, D. M. Rodrigues, "Influence of tool offsetting on the structure and morphology of dissimilar aluminum to copper friction-stir welds", Metallurgical and Materials Transactions A, **43(13)**, 5096−5105 (2012)
24. Y. Gao, K. Nakata, K. Nagatsuka, T.Matsuyama, Y. Shibata, M. Amano, "Microstructures and mechanical properties of friction stir welded brass/steel dissimilar lap joints at various welding speeds", Materials & Design, **90**, 1018–1025 (2016)
25. Z. Liu, S. Ji, X. Meng, "Joining of magnesium and aluminum alloys via ultrasonic assisted friction stir welding at low temperature", International Journal of Advanced Manufacturing Technology, **97**, 4127–4136 (2018)
26. Z. Barlas, H. Uzun, "Microstructure and mechanical properties of friction stir butt welded dissimilar Cu/CuZn30 sheets", Journal of Achievements in Materials and Manufacturing Engineering, **30 (2)**, 182– 186 (2008)
27. S. Li, Y. Chen, J. Kang, Y. Huang, J. A. Gianetto, L. Yin, "Interfacial microstructures and mechanical properties of dissimilar titanium alloy and steel friction stir butt-welds", Journal of Manufacturing Processes, **40**, 160–168 (2019)
28. S. Li, Y. Chen, X. Zhou, J. Kang, Y. Huang, H. Deng, "High-strength titanium alloy/steel butt joint produced via friction stir welding", Materials Letters, **234**, 155–158 (2019)
29. A. Wu, Z. Song, K. Nakata, J. Liao, L. Zhou, "Interface and properties of the friction stir welded joints of titanium alloy Ti6Al4V with aluminum alloy 6061", Materials & Design, **71**, 85–92 (2015)
30. C. J. Won, H. Liu, U. Kohsaku, H. Fujii, "Dissimilar friction stir welding of immiscible titanium and magnesium", Materialia, **7**, 100389 (2019)
31. H. B. Li, S. X. Yang, S. C. Zhang, B. B. Zhang, Z. H. Jiang, H. Feng, P. D. Han, J. Z. Li, "Microstructure evolution and mechanical properties of friction stir welding super austenitic stainless steel S32654", Materials & Design, **118**, 207–217 (2017)
32. S.D. Dhanesh Babu, P. Sevvel, R. Senthil Kumar, "Simulation of heat transfer and analysis of impact of tool pin geometry and tool speed during friction stir welding ofAZ80A Mg alloy plates", Journal of Mechanical Science and Technology, **34 (10)**, 4239 – 4250 (2020)
33. L. Yu, K. Nakata, J. Liao, "Microstructural modification and mechanical property improvement in friction stir zone of thixomolded AE42 Mg alloy", Journal of Alloys and Compounds, **480**, 340–346 (2009)
34. G.R. Argade, S. Shukla, K. Liu, R.S. Mishra, "Friction stir lap welding of stainless steel and plain carbon steel to enhance corrosion properties", Journal of Materials Processing Technology, **259**, 259–269 (2018).

 https://doi.org/10.37896/pd91.5/91531

ISSN: 0369-8963

35. M. Al-Moussawi, A.J. Smith, “Defects in Friction Stir Welding of Steel”, Metallography, Microstructure, and Analysis, **7**, 194–202 (2018)
36. D.K. Yaduwanshi, S. Bag, S. Pal, “On the Effect of Tool Offset in Hybrid-FSW of Copper-Aluminium Alloy”, Materials and Manufacturing Processes, **33**, 277–287 (2018)
37. H. Wang, K. Wang, W. Wang, L. Huang, P. Peng, H. Yu, “Microstructure and mechanical properties of dissimilar friction stir welded type 304 austenitic stainless steel to Q235 low carbon steel”, Materials Characterization, **155**, 109803 (2019)
38. P. Sevvel, C. Satheesh, “Role of tool rotational speed in influencing microstructural evolution, residual-stress formation and tensile properties of friction-stir welded AZ80A Mg alloy”, Materiali In Tehnologije, **52 (5)**, 607–614 (2018)
39. G. Sharma, D. K. Dwivedi, “Study on microstructure and mechanical properties of dissimilar steel joint developed using friction stir welding”, International Journal of Advanced Manufacturing Technology, **88**, 1299–1307 (2017)
40. Y. Zhao, S. Jiang, S. Yang, Z. Lu, K. Yan, “Influence of cooling conditions on joint properties and microstructures of aluminum and magnesium dissimilar alloys by friction stir welding”, International Journal of Advanced Manufacturing Technology, **83**, 673–679 (2016)
41. C. Tingey, A. Galloway, A. Toumpis, S. Cater, “Effect of Tool Centreline Deviation on the Mechanical Properties of Friction Stir Welded DH36 Steel”, Materials & Design, **65**, 896–906 (2015)
42. B. Yokesh Kumar, P. Sevvel, “Impact of speed of traverse during joining of CDA101 plates by FSW process”, Scientia Iranica, **29 (4)**, 1817-1827 (2022)
43. M. M. Swamy, S. Muthukumaran, K. Kiran, “A Study on Friction Stir Multi Spot Welding Techniques to Join Commercial Pure Aluminum and Mild Steel Sheets”, Transactions of The Indian Institute of Metals, **70**, 1221–1232 (2017)
44. O.P. Abolusoro, E. T. Akinlabi, “Effects of processing parameters on mechanical, material flow and wear behaviour of friction stir welded 6101-T6 and 7075-T651 aluminium alloys”, Manufacturing Review, 7, 1 (2020)
45. K. K. Babu, K. Panneerselvam, P. Sathiya, A. H. N. Haq, S. Sundarrajan, P. Mastanaiah and C. V. S. Murthy, “Effects of various tool pin profiles on mechanical and metallurgical properties of friction stir welded joints of cryorolled AA2219 aluminium alloy”, Metallurgical Research & Technology, **115**, 212 (2018)

 https://doi.org/10.37896/pd91.5/91531